

New Attempts to Synthesize Layered Double Hydroxides Intercalated with $\text{SO}_4^{2-}/\text{Cs}^+$ Using Co-Precipitation and Exchange Reactions

Anne R. Sotiles^a and Fernando Wypych^{✉*,a}

^aDepartamento de Química, Centro Politécnico, Universidade Federal do Paraná (UFPR), Jardim das Américas, CP 19032, 81531-980 Curitiba-PR, Brazil

Layered double hydroxides (LDHs) with the compositions $(\text{Cs}^+/\text{NH}_4^+)_{0.111}[\text{M}^{2+}_{0.667}\text{Al}_{0.333}(\text{OH})_{2.0}(\text{SO}_4)_{0.222}]$ ($\text{M}^{2+} = \text{Mn}, \text{Zn}$) and basal distance of ca. 11 Å were obtained by co-precipitating Mn/Al and Zn/Al sulfate salts with aqueous NH_3 , using excess of Cs_2SO_4 . $[\text{Mn}_{0.667}\text{Al}_{0.333}(\text{OH})_2]\text{Cl}_{0.333}\cdot n\text{H}_2\text{O}$ and $[\text{M}^{2+}_{0.667}\text{Al}_{0.333}(\text{OH})_2](\text{NO}_3)_{0.333}\cdot n\text{H}_2\text{O}$ ($\text{M}^{2+} = \text{Mn}, \text{Zn}$) were also synthesized by co-precipitation, presenting respective basal distances of 8.92 and 7.92 Å. After applying exchange reactions with excess of Cs_2SO_4 , materials with basal distances of ca. 11 Å were obtained, indicating the exchange of chloride and nitrate with sulfate, without incorporation of Cs^+ . When $\text{Na}^+_{0.111}[\text{M}^{2+}_{0.667}\text{Al}_{0.333}(\text{OH})_{2.0}(\text{SO}_4)_{0.222}]$ ($\text{M}^{2+} = \text{Mn}, \text{Zn}$) obtained by co-precipitation and having basal distances of ca. 11 Å was exchanged with excess of Cs_2SO_4 , the content of sulfate remained constant and Na^+ was partially replaced with Cs^+ , but the amount was lower, indicating the probable composition $(\text{Na}^+/\text{Cs}^+)_y[\text{M}^{2+}_{0.667}\text{Al}_{0.333}(\text{OH})_{2-y}(\text{SO}_4)_{y/2}(\text{SO}_4)_{0.222-(y/2)}]$ ($\text{M}^{2+} = \text{Mn}, \text{Zn}$), where some of the hydroxide anions were replaced with grafted SO_4^{2-} .

Keywords: layered double hydroxide, intercalation, exchange reactions, sulfate, cesium

Introduction

The removal of radioactive nuclides from contaminated waters is an important topic of research, especially after the Fukushima Daiichi nuclear power plant accident in 2011, which released large amounts of radioactive nuclides into the environment, especially the dangerous radioactive nuclide ^{137}Cs . Several methods of cesium intercalation in layered materials have been reported in the literature, such in graphite,¹ 2H-NbS_2 ,² C-60,³ 1T-TaSe_2 ,⁴ manganese thiophosphate,⁵ clay minerals,⁶ 1T-MoS_2 ,⁷ sulfate green rusts (GR_{SO_4}) with the formula $\text{NaFe}^{\text{II}}_6\text{Fe}^{\text{III}}_3(\text{SO}_4)_2(\text{OH})_{18}\cdot 12\text{H}_2\text{O}$ ⁸ clay minerals from the smectite group,⁶ and other clay minerals,⁹⁻¹¹ but to the best of our knowledge, none of them have reported the intercalation of cations in layered double hydroxides (LDH), especially due to the fact that LDHs are typically anion exchangers.

Traditional LDH with the chemical composition $[\text{M}^{2+}_{1-x}\text{M}^{3+}_x(\text{OH})_2](\text{A}^{n-})_{x/n}\cdot n\text{H}_2\text{O}$ are natural minerals and synthetic materials derived from the brucite-like structure ($\text{Mg}(\text{OH})_2$), in which M^{2+} octahedrally coordinated to six

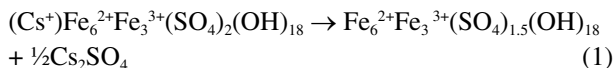
OH^- anions share edges to form two-dimensional layers that are stacked in the basal direction. In the LDH structure, M^{2+} cations in the brucite-like structure are partially replaced by M^{3+} and the excess positive charges of the layers are compensated by the intercalation of normally hydrated A^{n-} anions.¹²⁻²⁰

Recently, it has also been reported that LDHs can be obtained with the chemical composition $(\text{D}(\text{H}_2\text{O})_6)[\text{M}^{2+}_6\text{Al}_3(\text{OH})_{18}(\text{SO}_4)_2]\cdot 6\text{H}_2\text{O}$ ($\text{D}^+ = \text{Li}, \text{Na}$ or K and $\text{M}^{2+} = \text{Mn}, \text{Zn}, \text{Mg}, \text{Co}, \text{Ni}, \text{Cu}$). These compounds were intercalated with hydrated sulfate anions, alkali metal cations and ammonium.²¹⁻²⁴ Although the synthetic phases involved the intercalation of $\text{Li}^+, \text{Na}^+, \text{K}^+$ and NH_4^+ , the minerals containing $\text{M}^{2+}/\text{Al}^{3+}$ in the molar ratio of 2:1 were reported only with the intercalation of Na^+ (natroglaucocerinite- $\text{M}^{2+} = \text{Zn}$; shigaite- $\text{M}^{2+} = \text{Mn}$ and motukoreaite- $\text{M}^{2+} = \text{Mg}$).²⁵⁻²⁸ Other phases have also been reported with the compositions $\text{Fe}^{2+}/\text{Fe}^{3+}$, like nikischerite and sodium sulfate green rusts.^{8,29,30} In fact, nikischerite and sulfate green rusts have the same composition $[\text{NaFe}^{2+}_6\text{Fe}^{3+}_3(\text{SO}_4)_2(\text{OH})_{18}(\text{H}_2\text{O})_{12}]$ and also similar lattice parameters (nikischerite: $a = b = 9.347$ Å, $c = 33.00$ Å and sulfate green rust: $a = b = 9.258$ Å, $c = 10.968$ Å), but they occur in different polytypes, which differ only in the number of stacked layers in the unit cell.²⁹⁻³¹

*e-mail: wypych@ufpr.br

Editors handled this article: Jaisa Fernandes Soares and Pedro H. C. Camargo (Associate)

Only sulfate green rusts have Cs⁺ and Rb⁺ intercalated together with sulfate anions,⁸ but washing of the materials with water indicated that Na⁺ and K⁺ were not affected, while Rb⁺ and Cs⁺ were leached out of the structure, with the corresponding reduction of the amount of intercalated sulfate and the basal distance. The reaction can be probably formulated as described in equation 1, when the cesium sulfate green rusts are converted into regular LDH.



Due to the possibility to extend the broad range of applications of LDH, especially related to the possibility to remove radioactive Cs⁺ from contaminated solutions and the lack of data about the intercalation of Cs⁺ in LDH/SO₄, the objective of the present work is to describe attempts to synthesize and characterize Zn/Al and Mn/Al LDH containing SO₄²⁻/Cs⁺, obtained by co-precipitation at increasing pH and exchange reactions.

Experimental

The synthesis of Mn₂Al:Cl, Mn₂Al:NO₃ and Zn₂Al:NO₃ phases was performed as recently reported.²¹ Briefly, LDH containing M²⁺:Al with molar ratios of 2:1 were synthesized by co-precipitation with increasing pH using an automatic glass titration reactor operating at 90 °C, under N₂ flow, to avoid contamination with carbonate, where the pH was controlled by an internal pHmeter. A 100 mL solution of MnCl₂/AlCl₃, Mn(NO₃)₂/Al(NO₃)₃ or Zn(NO₃)₂/Al(NO₃)₃ were prepared with Milli-Q water and slowly titrated with a solution of NaOH 1 mol L⁻¹, until attaining the desired pH. In the absence of CsOH to perform the co-precipitation, the M²⁺₂Al:SO₄/Cs (M²⁺ = Mn, Zn) samples were also synthesized by adding aqueous NH₃ 1 mol L⁻¹ solutions to 200 mL solutions of M²⁺SO₄ (M²⁺ = Mn, Zn), Al₂(SO₄)₃ and

Cs₂SO₄ prepared with Milli-Q water, with M²⁺:Al metal molar ratios of 2:1 using an excess of Cs₂SO₄ (Table 1).

All the chemicals were of analytical grade and used without any treatment: Al₂(SO₄)₃·16H₂O 98-102%, NaOH 99%, Al(NO₃)₃·9H₂O 98.50%, Mn(NO₃)₂·4H₂O 98%, Li₂SO₄·H₂O 99%, ZnSO₄·7H₂O 99% and NaCl 99.85% were from Reatec (São Paulo, Brazil); AlCl₃·6H₂O 99.50%, MnCl₂·4H₂O 98-101%, ZnCl₂ Vetec 97% and Zn(NO₃)₂·6H₂O 99% were from Vetec (Rio de Janeiro, Brazil); LiOH·H₂O Biotec 98% (São Paulo, Brazil); Na₂SO₄ Neon 99.9% (São Paulo, Brazil); NaNO₃ F. Maia 99% (São Paulo, Brazil); Aqueous NH₃ Quimex 28-30% (Minas Gerais, Brazil); MnSO₄·H₂O Alphatec 98-101% (Rio de Janeiro, Brazil); Cs₂SO₄ Merck 99.9% (Darmstadt, Germany).

After precipitation, the resulting slurries were ripened at 90 °C for 5 days in closed Erlenmeyer flasks, and separated by centrifugation at 4,000 rpm for 5 min (centrifugal force of 2,125 g), with the process being repeated after redispersing the slurry with an ultrasound bath for several seconds.²² The samples were dried at room temperature. The M²⁺₂Al:SO₄/Na, M²⁺₂Al:NO₃ (M²⁺ = Mn, Zn) and Mn₂Al:Cl samples were synthesized as previously reported.^{21,22}

In the exchange reactions, the phases Mn₂Al:SO₄/Na, Zn₂Al:SO₄/Na, Mn₂Al:NO₃, Zn₂Al:NO₃ and Mn₂Al:Cl were dispersed in Milli-Q water containing excess of Cs₂SO₄ (three times the sulfate in relation of nitrate and chloride and three times in relation to sodium), and the mixtures were gently stirred for 7 days under N₂ flow at room temperature. The same procedure was used in the centrifugation washing and drying process of the other samples. In all exchanged samples, the pH was kept almost constant and close to neutral (in the range of 6.7 to 7.7).

The synthesized compounds were characterized by X-ray diffraction (XRD) using a Shimadzu XRD-6000 diffractometer (Kyoto, Japan). After aging and the last centrifugation step, drops of the slurry were deposited on glass sample holders and dried at room temperature. The analyses were performed using Cu Kα = 1.5418 Å

Table 1. Amount of chemicals used and pH control during the LDH syntheses

Compound	M ²⁺ SO ₄ / mmol	Al ₂ (SO ₄) ₃ / mmol	D ₂ SO ₄ / mmol	Initial pH	Final pH
Zn ₂ Al:SO ₄ /Cs	14.700	3.675	3.650	3.54	9.48
Mn ₂ Al:SO ₄ /Cs	15.493	3.873	3.871	3.89	8.98
Mn ₂ Al:SO ₄ /Na	26.186	6.551	2.188	3.43	9.06
Zn ₂ Al:SO ₄ /Na	24.783	6.418	2.007	3.46	9.51
Compound	M ²⁺ B ₂ / mmol	AlB ₃ / mmol	NaB / mmol	Initial pH	Final pH
Mn ₂ Al:NO ₃	24.922	12.448	4.168	3.07	9.06
Mn ₂ Al:Cl	27.372	13.714	4.560	3.15	9.11
Zn ₂ Al:NO ₃	31.071	15.509	5.179	2.88	9.31

M²⁺ = Mn or Zn; D = Na⁺ or Cs⁺; B = NO₃⁻ or Cl⁻.

radiation, tension of 40 KV and current of 30 mA, with a dwell time of 2° min^{-1} .

The samples were also characterized by Fourier transform infrared (FTIR) spectroscopy using a Bruker Vertex 70 spectrophotometer (Karlsruhe, Germany). KBr pellets containing around 1% (m/m) of LDH were gently mixed and pressed at 10 tons and the spectra were collected in transmission mode by accumulating 32 scans in the region of $400\text{--}4000 \text{ cm}^{-1}$, using resolution of 2 cm^{-1} .

Scanning electron microscopy (SEM) images and energy dispersive X-ray spectroscopy (EDS) data of some precursors were obtained with a Tescan Vega3LMU microscope (Brno-Kohoutovice, Czech Republic) with an AZ Tech software. The sample dispersions in water were dripped on copper tapes and after EDS measurements, the samples were sputtered with a thin gold layer to obtain the SEM images.

The quantitative analyses of the metals and sulfur (relative to SO_4^{2-}) used to formulate the samples' chemical composition were performed with a Thermo Scientific model iCAP 6500 inductively coupled plasma optical emission spectrometry (ICP-OES) (Waltham, United States) after dissolving the samples in 1.0% v/v of HNO_3 in Milli-Q water. The data were collected in triplicate, treated with the Thermo Scientific iTeva software version 1.2.0.30 and average values were used to obtain the LDH compositions.

Results and Discussion

In general, during exchange reactions, the layer lattice parameters remain almost constant while the basal parameter is normally dependent on the size of the intercalated cations and/or anions. During these reactions, it is also common for interpolytype transitions to occur due to the re-ordering of the layer stacking sequence. However, this seems not to be the case of exchange reactions of $(\text{D}_1^+)[\text{M}^{2+}_6\text{Al}_3(\text{OH})_{18}(\text{SO}_4)_2]$ to $(\text{D}_2^+)[\text{M}^{2+}_6\text{Al}_3(\text{OH})_{18}(\text{SO}_4)_2]$

(D_1^+ and D_2^+ = alkali metal cations), since the basal distance is obtained by the combination of different factors: the hydrated sulfate size in the form of a double layer; the size of the hydrated alkali metal cations with variable numbers of water molecules in the first hydration shell; and also to the interactions of sulfate with the alkali metal, water molecules and both with the layers having different compositions.

The samples $\text{Mn}_2\text{Al}:\text{SO}_4/\text{Cs}$ (Figure 1Aa) and $\text{Zn}_2\text{Al}:\text{SO}_4/\text{Cs}$ (Figure 1Ab) obtained by co-precipitation presented, respectively, basal distances of 11.36 and 10.91 Å. $\text{Zn}_2\text{Al}:\text{SO}_4/\text{Cs}$ (Figure 1Ab) also was slightly contaminated with compounds having a basal distance of 8.9 Å, exactly the same impurity observed when $\text{Zn}_2\text{Al}:\text{SO}_4/\text{NH}_4$ was prepared,²⁴ attributed probably to the intercalation of dehydrated sulfate.^{32,33}

The values of the prevalent compounds are slightly bigger than those obtained for the $\text{Mn}_2\text{Al}:\text{SO}_4$ phases intercalated with sodium (11.02–11.03 Å) and potassium (11.27–11.28 Å) and slightly smaller than those observed for $\text{Zn}_2\text{Al}:\text{SO}_4$ phases intercalated with sodium (11.22–11.14 Å) and potassium (11.40 Å). Both values are consistent with the intercalation of sulfate in double layer arrangement and a single layer of hydrated Cs^+ and NH_4^+ , as observed for other alkali metal cations.²⁴

An expansion of the XRD pattern of $\text{Mn}_2\text{Al}:\text{SO}_4/\text{Cs}$ (Figure 1Aa, insert) presents the (100; $d = 4.80 \text{ Å}$) and (101; $d = 4.42 \text{ Å}$) diffraction peaks, which correspond to an $a = a' \sqrt{3}$ superlattice, common for LDH with $2\text{M}^{2+}:\text{M}^{3+}$ molar ratios intercalated with different anions and also observed in LDH intercalated with sulfate and alkali metal cations,^{21,22} attributed to the ordering of metal cations in the layers. The cell parameters were calculated and found to be $a = b = 5.54 \text{ Å}$ and $c = 11.36 \text{ Å}$ with average distance between the metals of $a' = 3.20 \text{ Å}$, very close to $a' = 3.171 \text{ Å}$ observed in the sodium shigaite structure.²⁸ The same was not observed for $\text{Zn}_2\text{Al}:\text{SO}_4/\text{Cs}$ due to the overlapping of the second peak of the 8.9 Å phase, in the same region.

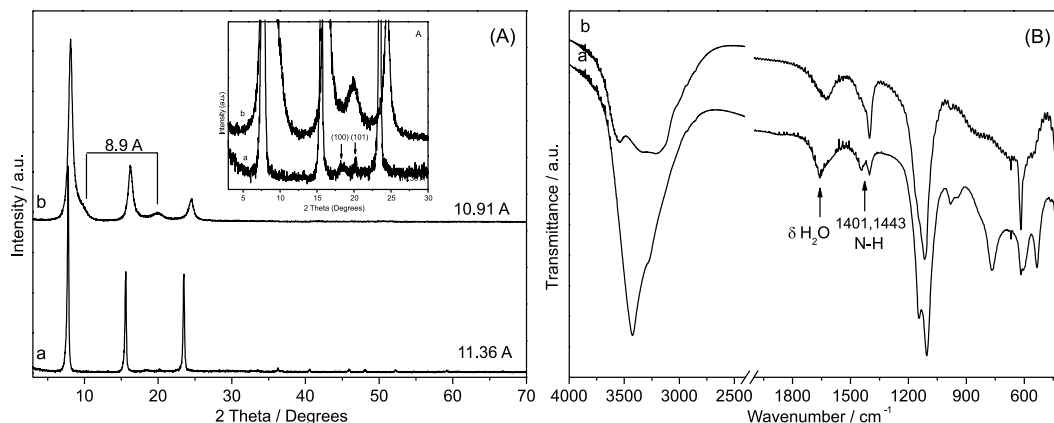


Figure 1. XRD patterns (A) and FTIR spectra (B) of $\text{Mn}_2\text{Al}:\text{SO}_4/\text{Cs}$ (a) and $\text{Zn}_2\text{Al}:\text{SO}_4/\text{Cs}$ (b) obtained by co-precipitation with increasing pH.

Although the $a = a' \sqrt[3]{} \times a \sqrt[3]{}$ superstructure is also observed in synthetic LDHs intercalated with sulfate and alkali metal cations,^{21,22} natural LDHs intercalated with sulfate and alkali metal cations present the superstructure $a = 3a' \times 3a'$, which correspond to the ordering of the metal cations and/or sulfate anions between the layers.²⁸⁻³² These superstructure differences are probably associated with the sizes of the crystals and corresponding long and short-range order/disorder in synthetic and natural LDH. Since the basal distances are similar, the hydration shell of the intercalated alkali metal cations and ammonium should be different from those observed in solution, being respectively tetrahedral and octahedral for Li^+ , octahedral for Na^+ , square antiprismatic for K^+ and Rb^+ , probably 12-coordinated for Cs^+ ³⁴ and not well established for NH_4^+ , for which the number of water molecules in the hydration shell ranges from 4 to 6.^{35,36}

The average thicknesses of the particles along the basal axis and the respective number of stacked layers were calculated by the Scherrer equation using the first basal peak. The data correspond to 13.5 and 41 nm, respectively, for $\text{Mn}_2\text{Al}:\text{SO}_4/\text{Cs}$ and $\text{Zn}_2\text{Al}:\text{SO}_4/\text{Cs}$, which corresponds to 12 and 36 stacked layers, respectively.

The presence of ammonium was inferred since the precipitation was conducted with aqueous NH_3 instead of CsOH , so no other cations were available in the alkaline solution to explain the higher content of sulfate anions. Although hydrated SO_4^{2-} and NH_4^+ were intercalated between the layers, the basal distance was only slightly affected in comparison to the other sulfate/alkali metal cations.

The FTIR spectra of $\text{Mn}_2\text{Al}:\text{SO}_4/\text{Na}$ (Figure 1Ba) and $\text{Zn}_2\text{Al}:\text{SO}_4/\text{Na}$ (Figure 1Bb) indicated the presence of typical stretching vibration bands of hydroxyl groups and water molecules in the region of 3430 cm^{-1} , sulfate bands and M–O and M–OH bands below 600 cm^{-1} and a band in the region of $770\text{--}790\text{ cm}^{-1}$. The absorption band in the region of 1620 cm^{-1} is attributed to the bending vibration of water molecules.^{21-24,37}

Due to different compositions and metals involved in the structure, the FTIR bands attributed to M–O and M–OH bonds were observed at 419, 534 and 767 cm^{-1} for $\text{Mn}_2\text{Al}:\text{SO}_4/\text{Cs}$ (Figure 1Ba), while only two bands, at 427 and 617 cm^{-1} , were observed for $\text{Zn}_2\text{Al}:\text{SO}_4/\text{Cs}$ (Figure 1Bb). This absence can be attributed to the mixture of phases and low crystallinity of $\text{Zn}_2\text{Al}:\text{SO}_4/\text{Cs}$ in comparison with $\text{Mn}_2\text{Al}:\text{SO}_4/\text{Cs}$. The sulfate bands in distorted tetrahedral symmetry also changed positions, being observed as a broad band at 1116 and 617 cm^{-1} for $\text{Zn}_2\text{Al}:\text{SO}_4/\text{Cs}$ (Figure 1Bb) and at 1145, 1105, 981, 617 and 606 cm^{-1} for $\text{Mn}_2\text{Al}:\text{SO}_4/\text{Cs}$ (Figure 1Ba). The presence of

typical N–H bending vibration bands with low-symmetry ammonium was detected by FTIR in both samples at 1401 and 1443 cm^{-1} , along with a low-intensity O–H overlapping band in the region of $3000\text{--}3700\text{ cm}^{-1}$.^{24,35,38} The band splitting in the region of 1400 cm^{-1} is probably related to hydrogen bonding occurring between NH_4^+ ions and H_2O molecules and interactions with the negatively charged layers $[\text{M}^{2+}_6\text{Al}_3(\text{OH})_{18}(\text{SO}_4)_2]^-$. In solid NH_4Cl , the band in the region of 1400 cm^{-1} is attributed to symmetric deformation mode ν_4 of tetrahedral ammonium symmetry,^{39,40} and this band was also observed at 1450 cm^{-1} when NH_4^+ was in solution.

The composition of the synthesized sample (Table 2) indicated that the observed values for the M^{2+} and M^{3+} metals in $\text{Zn}_2\text{Al}:\text{NO}_3$, $\text{Mn}_2\text{Al}:\text{NO}_3$ and $\text{Mn}_2\text{Al}:\text{Cl}$ were almost identical to the expected ideal formulas $[\text{M}^{2+}_{0.667}\text{Al}^{3+}_{0.333}(\text{OH})_2](\text{A}^-)_{0.333}n\text{H}_2\text{O}$, according to the proportions used during the synthesis procedures (Table 1), with the exception of $\text{Zn}_2\text{Al}:\text{SO}_4/\text{Cs}$, which indicated a slightly higher content of Al^{3+} , due to the presence of impurities (Figure 1Ab) (0.372 instead of 0.333).

The same observation occurred after the exchange reaction of $\text{Zn}_2\text{Al}:\text{SO}_4/\text{Na}$ with Cs_2SO_4 (0.367 instead of 0.333). The chemical composition of the phases $\text{Zn}_2\text{Al}:\text{SO}_4/\text{Cs}$ and $\text{Mn}_2\text{Al}:\text{SO}_4/\text{Cs}$ obtained by direct synthesis also indicated the correct proportions of M^{2+} and M^{3+} and sulfur from sulfate for the ideal composition $\text{Cs}^+_{0.111}[\text{M}^{2+}_{0.667}\text{Al}_{0.333}(\text{OH})_2](\text{SO}_4)_{0.222}$, but the content of cesium was lower than predicted.

Although not quantified, this difference can be attributed to NH_4^+ , as indicated by FTIR (Figure 1Ba,b), since the precipitation was conducted in the presence of aqueous NH_3 and $\text{NH}_4^+/\text{SO}_4^{2-}$. Intercalated LDH have already been reported in the literature, having similar basal distances.²⁴ These compositions are proposed to be $(\text{Cs}_{0.111-x}\text{NH}_4^+_x)[\text{M}^{2+}_{0.667}\text{Al}_{0.333}(\text{OH})_2](\text{SO}_4)_{0.222}$.

The reduced content of intercalated Cs^+ and Rb^+ have already been reported for sulfate green rusts (GR_{SO_4}), having chemical composition close to $\text{D}^+\text{Fe}^{\text{II}}_6\text{Fe}^{\text{III}}_3(\text{SO}_4)_2(\text{OH})_{18} \cdot 12\text{H}_2\text{O}$ ($\text{D}^+ = \text{Na}, \text{K}, \text{Rb}, \text{Cs}$),⁸ while rinsed samples of intercalated cesium were observed to have smaller basal distance (10.85 \AA) than sodium (10.96 \AA) and potassium (11.20 \AA), in spite of the bigger ionic radius of the first. A single washing step was sufficient to remove all intercalated Cs^+ from GR_{SO_4} , and only a double layer of sulfate was retained.⁸ This behavior was not observed in our samples, in which cesium was still observed despite being washed twice, indicating a stronger interaction with the LDH layers.

In the attempt to exchange Na^+ from $\text{Mn}_2\text{Al}:\text{SO}_4/\text{Na}$ and $\text{Zn}_2\text{Al}:\text{SO}_4/\text{Na}$ with Cs^+ , again the content of Cs^+ plus

Table 2. Composition of the samples obtained by ICP-OES analyses

Sample	M^{2+}	Al^{3+}	B^-	Na^+
	0.667 ^a	0.333 ^a	0.333 ^a	0.00 ^a
$\text{Zn}_2\text{Al}:\text{NO}_3$	0.665	0.335	n.e.	0.00
$\text{Mn}_2\text{Al}:\text{NO}_3$	0.670	0.330	n.e.	0.00
$\text{Mn}_2\text{Al}:\text{Cl}$	0.662	0.338	n.e.	0.00
Sample	M^{2+}	Al^{3+}	SO_4^{2-}	$\text{D} = \text{Na}^+, \text{Cs}^+ \text{ or } \text{NH}_4^+$
	0.667 ^b	0.333 ^b	0.222 ^b	0.111 ^b
$\text{Zn}_2\text{Al}:\text{SO}_4/\text{Cs}$	0.628	0.372	0.246	0.023 (0.088 ^c)
$\text{Mn}_2\text{Al}:\text{SO}_4/\text{Cs}$	0.646	0.354	0.242	0.014(0.097 ^c)
$\text{Mn}_2\text{Al}:\text{SO}_4/\text{Na}$	0.661	0.339	0.223	0.121
$\text{Zn}_2\text{Al}:\text{SO}_4/\text{Na}$	0.645	0.355	0.217	0.099
$\text{Mn}_2\text{Al}:\text{SO}_4/\text{Na-Cs}$	0.660	0.340	0.220	$\text{Na} = 0.015; \text{Cs} = 0.036$
$\text{Zn}_2\text{Al}:\text{SO}_4/\text{Na-Cs}$	0.633	0.367	0.239	$\text{Na} = 0.067; \text{Cs} = 0$
Sample	M^{2+}	Al^{3+}	SO_4^{2-}	$\text{D} = \text{Na}^+, \text{Cs}^+ \text{ or } \text{NH}_4^+$
	0.667 ^d	0.333 ^d	0.167 ^d	0.00 ^d
$\text{Mn}_2\text{Al}:\text{NO}_3/\text{Cs}$	0.659	0.341	0.167	0.027
$\text{Zn}_2\text{Al}:\text{NO}_3/\text{Cs}$	0.663	0.337	0.146	0.000
$\text{Mn}_2\text{Al}:\text{Cl}/\text{Cs}$	0.667	0.333	0.150	0.025

^aExpected value of $[\text{M}^{2+}_{0.667}\text{Al}^{3+}_{0.333}(\text{OH})_2](\text{B}^-)_{0.333}\cdot\text{nH}_2\text{O}$ ($\text{B}^- = \text{NO}_3^-$ or Cl^-). ^bExpected values of $\text{D}_{0.111}[\text{M}^{2+}_{0.667}\text{Al}_{0.333}(\text{OH})_2](\text{SO}_4)_{0.222}$. ^cPredicted content of NH_4^+ ; $\text{D} = \text{Na}^+, \text{Cs}^+ \text{ or } \text{NH}_4^+$. ^dExpected values of $[\text{M}^{2+}_{0.667}\text{Al}_{0.333}(\text{OH})_2](\text{SO}_4)_{0.167}$. n.e.: not evaluated.

Na^+ did not have the expected value, and the content of sulfate was again higher, suggesting the maintenance of the original composition $\text{D}^+_{0.111}[\text{M}^{2+}_{0.667}\text{Al}_{0.333}(\text{OH})_2](\text{SO}_4)_{0.222}$. HSO_4^- is not expected at neutral and slightly alkaline pH,⁴¹ since this would increase the amount of sulfur in the samples and the absence of other cations in solution, an alternative is to consider that part of the alkali metal cations was replaced with hydrated protons. However, this hypothesis is unlikely since the pH of the exchange solution was neutral or slightly alkaline.

The second possibility is the adsorption of sulfate on the protonated hydroxide anions of the particles' surface through $-\text{OH}_2^+(\text{SO}_4^{2-})_{0.5}$.⁴¹ However, it is highly unlikely that the exact amount proposed in the ideal formula $\text{D}^+_{0.111}[\text{M}^{2+}_{0.667}\text{Al}_{0.333}(\text{OH})_2](\text{SO}_4)_{0.222}$ would be obtained.

A third and more feasible hypothesis is the grafting of sulfate, as observed in layered hydroxide salts like sodium gordaite ($\text{NaZn}_4(\text{OH})_6(\text{SO}_4)\text{Cl}\cdot 6\text{H}_2\text{O}$),^{42,43} where part of the structural hydroxide anions is replaced and grafted with chloride and sulfate, generating negatively charged layers $[\text{Zn}_4(\text{OH})_6(\text{SO}_4)\text{Cl}]^-$, whose charges are compensated by the intercalation of Na^+ cations. Although bereft of alkali metal cations, layered double hydroxides with the proposed grafting mechanism have similar structures to spangolite ($\text{Cu}_6\text{Al}(\text{OH})_{12}(\text{SO}_4)\text{Cl}\cdot 3\text{H}_2\text{O}$)⁴⁴ and jaborite ($\text{Ni}^{2+}_{1-x}\text{Co}^{3+}_x(\text{OH})_{2-x}(\text{SO}_4)_x\cdot\text{nH}_2\text{O}$),⁴⁵ where the SO_4^{2-} tetrahedra are grafted to the layer, partially replacing surface OH^- . Using the structures of jaborite (where

sulfate is grafted to the layers) and zincowoodwardite ($[\text{Zn}_{1-x}\text{Al}_x(\text{OH})_2][(\text{SO}_4)_{x/2}\cdot\text{nH}_2\text{O}]^{46}$ (where sulfate is only intercalated) as examples, and with $x = 0.333$, the formulas would be $\text{Ni}^{2+}_{0.667}\text{Co}^{3+}_{0.333}(\text{OH})_{1.667}(\text{SO}_4)_{0.333}\cdot\text{nH}_2\text{O}$ and $\text{Zn}_{0.667}\text{Al}^{3+}_{0.333}(\text{OH})_2(\text{SO}_4)_{0.167}\cdot\text{nH}_2\text{O}$.

In jaborite, the content of sulfate would double in relation to zincowoodwardite while the $\text{M}^{2+}:\text{M}^{3+}$ ratio would be the same (2:1). Grafting of sulfate and carbonate has even been observed in single hydroxides, as is in the case of paraotwayite ($\text{Ni}(\text{OH})_{2-x}(\text{SO}_4, \text{CO}_3)_{x/2}$)⁴⁷ and was also in LDH intercalated with dehydrated sulfate.^{32,33} Hence, it would not be surprising to find this pattern in LDH intercalated with hydrated sulfate.

Using $x = 0.333$ and $y = 0.50$ in the formula $\text{D}^+_y[\text{M}^{2+}_{1-x}\text{Al}_x(\text{OH})_{2-y}(\text{SO}_4)_{y/2}(\text{SO}_4)_{0.222-(y/2)}]$ as an example (reduction of the content of alkali metal cations of 50%) in relation to the shigaite-like formula $\text{Cs}[\text{M}^{2+}_6\text{Al}_3(\text{OH})_{18}(\text{SO}_4)_{2.0}]$ and keeping the metal molar ratio of 2:1, LDHs with the composition $(\text{Cs})_{0.50}[\text{M}^{2+}_6\text{Al}_3(\text{OH})_{17.5}(\text{SO}_4)_{0.25^*}(\text{SO}_4)_{1.75}]$ would be obtained, which in a reduced way would be formulated as $(\text{Cs})_{0.056}[\text{M}^{2+}_{0.667}\text{Al}_{0.333}(\text{OH})_{1.944}(\text{SO}_4)_{0.028^*}(\text{SO}_4)_{0.194}]$ (total $\text{SO}_4^{2-} = 0.222$ and $*$ = grafted SO_4^{2-}) or even $(\text{Cs})_{0.056}[\text{M}^{2+}_{0.667}\text{Al}_{0.333}(\text{OH})_{1.944}(\text{SO}_4)_{0.222}]$.

These propositions where some of hydroxide anions from the layers are replaced and grafted with SO_4^{2-} are in relatively good agreement with the formulas suggested by the ICP-OES analyses (Table 2).

The XRD patterns and FTIR spectra before and after exchange reactions are shown in Figure 2. When the samples $\text{Mn}_2\text{Al}:\text{SO}_4/\text{Na}$ (Figure 2Aa) and $\text{Zn}_2\text{Al}:\text{SO}_4/\text{Na}$ (Figure 2Ac) were exchanged with Cs_2SO_4 , the basal distances remained almost constant in both cases (11.04 to 11.15 Å for $\text{Zn}_2\text{Al}:\text{SO}_4/\text{Na}$ (Figure 2Aa,c) and 11.15 to 11.14 Å for $\text{Mn}_2\text{Al}:\text{SO}_4/\text{Na}$ (Figure 2Ab,d). This indicates that the exchange reaction was unsuccessful, since the basal distances observed for the samples of $\text{Mn}_2\text{Al}:\text{SO}_4/\text{Cs}$

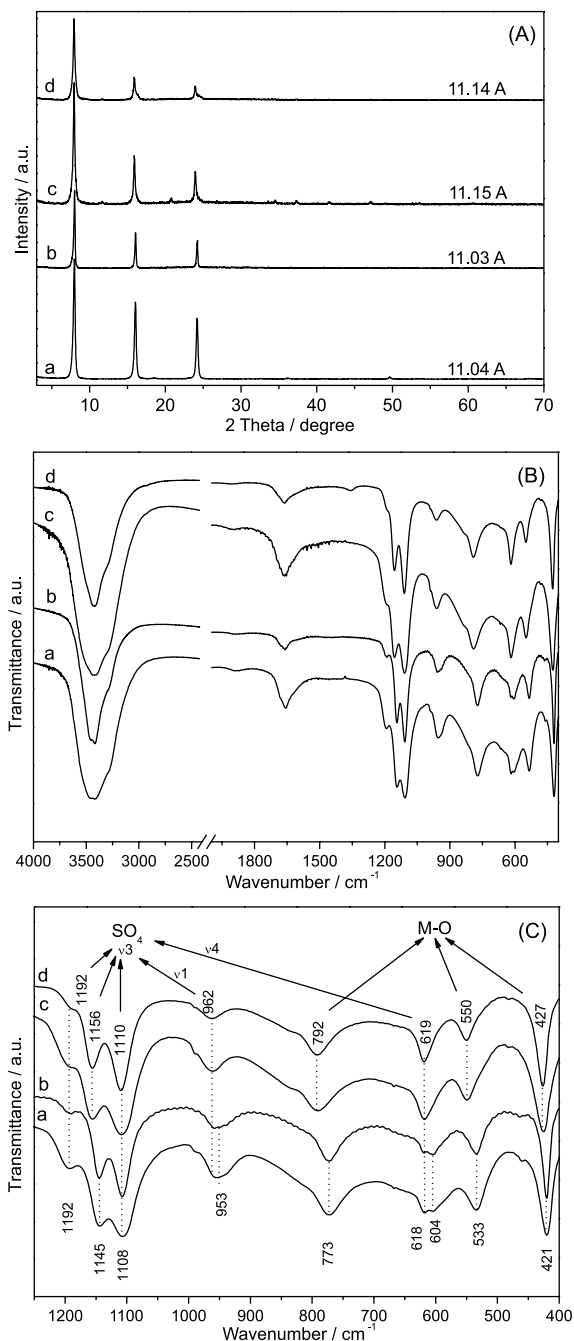


Figure 2. XRD patterns (A) and FTIR spectra (B, C) of $\text{Mn}_2\text{Al}:\text{SO}_4/\text{Na}$ (a) and $\text{Zn}_2\text{Al}:\text{SO}_4/\text{Na}$ (c) and after respective exchange reactions with Cs_2SO_4 : $\text{Mn}_2\text{Al}:\text{SO}_4/\text{Na-Cs}$ (b) and $\text{Zn}_2\text{Al}:\text{SO}_4/\text{Na-Cs}$ (d).

(Figure 1Aa) and $\text{Zn}_2\text{Al}:\text{SO}_4/\text{Cs}$ (Figure 1Ab) obtained by co-precipitation were also in the same range (11.36 Å for $\text{Mn}_2\text{Al}:\text{SO}_4/\text{Cs}$ and 10.91 Å for $\text{Zn}_2\text{Al}:\text{SO}_4/\text{Cs}$).

When the FTIR spectra were evaluated, the same band positions were observed in the samples before and after exchange reactions, with Cs_2SO_4 , at 1192, 1145, 1108, 953, 773, 618, 604, 533 and 421 cm^{-1} for $\text{Mn}_2\text{Al}:\text{SO}_4/\text{Cs}$ (Figure 2Ca,b) and at 1192, 1156, 1110, 962, 792, 619, 550, 427 cm^{-1} for $\text{Zn}_2\text{Al}:\text{SO}_4/\text{Cs}$ (Figure 2Cc,d). This observation is different than that of washed samples of green rusts intercalated with cesium and rubidium, when the removal of the cations was attributed to shifting of the ν_3 bands of sulfate at about 15 cm^{-1} to lower wavenumbers.⁸

The presence of the split band in the region of 1100 cm^{-1} in all samples suggests that the sulfate environment is highly distorted,³⁷ since in the absence of sulfate/alkali metal/layer interaction, sulfate's undistorted tetrahedral symmetry would be characterized by a single band in the region of 1100 cm^{-1} .⁴⁸ Grafting of SO_4^{2-} would only contribute to very low intensity bands in the same region,³² which were overlapped by the other sulfate bands. More details of the band attributions can be found in the literature.⁴⁸ Figure 3A shows the results of our attempt to produce the phases intercalated with sulfate and cesium, using the precursor $\text{Mn}_2\text{Al}:\text{NO}_3$ (Figure 3Aa), $\text{Zn}_2\text{Al}:\text{NO}_3$ (Figure 3Ac) and $\text{Mn}_2\text{Al}:\text{Cl}$ (Figure 3Ae).

As expected, in all cases after the attempts to exchange the pristine anions with $\text{SO}_4^{2-}/\text{Cs}^+$, we found that the basal distances increased from 8.92 Å in $\text{Mn}_2\text{Al}:\text{NO}_3$ (Figure 3Aa) and $\text{Zn}_2\text{Al}:\text{NO}_3$ (Figure 3Ac) to around 11 Å, and from 7.82 Å in $\text{Mn}_2\text{Al}:\text{Cl}$ (Figure 3Ae)^{32,49} also to around 11 Å (Figure 3Ab,d,f), indicating that the former's intercalated anions were replaced with SO_4^{2-} ,^{21,37} but not with $\text{SO}_4^{2-}/\text{Cs}^+$, as already indicated by the ICP-OES analyses (Table 2).

This is evidence that $\text{Cs}^+/\text{SO}_4^{2-}$ are not stable phases that can be obtained by exchange reactions, as already reported for sulfate green rusts,⁸ but this is not true in the case of exchanging the same LDH with Li^+ , Na^+ and K^+ , where the exchange reactions were successful.²¹ More studies are still necessary to explain this instability also for LDHs intercalated with $\text{Rb}^+/\text{SO}_4^{2-}$.

It has also been reported in the literature that sulfate contains several degrees of hydration and those with 11 Å correspond to double hydration. Lower basal distances and interpolytypic transitions can be obtained by heating or submitting the samples to dry air or vacuum.^{33,50-52} However, our samples were dried at room temperature and no changes of the basal distances were observed (they remained close to 11 Å). The obtention of exchanged compounds having the basal distance of 10.94 Å for $\text{Mn}_2\text{Al}:\text{NO}_3/\text{Cs}$ (Figure 3Ab), 11.00 Å for $\text{Zn}_2\text{Al}:\text{NO}_3/\text{Cs}$ (Figure 3Ad) and

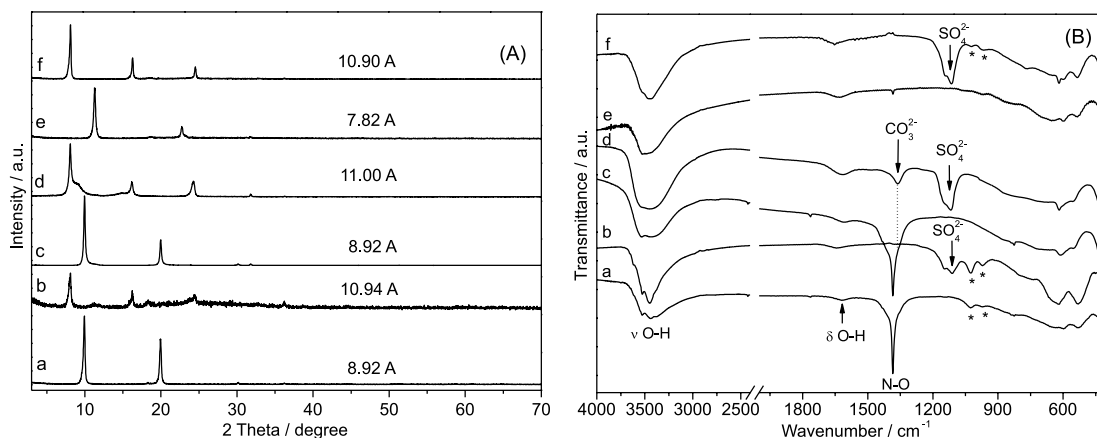


Figure 3. XRD patterns (A) and FTIR spectra (B) of $\text{Mn}_2\text{Al}:\text{NO}_3$ (a), $\text{Zn}_2\text{Al}:\text{NO}_3$ (c) and $\text{Mn}_2\text{Al}:\text{Cl}$ (e) and after respective exchange with $\text{Cs}_2\text{SO}_4:\text{Mn}_2\text{Al}:\text{NO}_3/\text{Cs}$ (b), $\text{Zn}_2\text{Al}:\text{NO}_3/\text{Cs}$ (d) and $\text{Mn}_2\text{Al}:\text{Cl}/\text{Cs}$ (f).

10.90 Å for $\text{Mn}_2\text{Al}:\text{Cl}/\text{Cs}$ (Figure 3Af) is an indication that the compounds are similar to those obtained with the direct synthesis (11.36 Å for $\text{Mn}_2\text{Al}:\text{SO}_4/\text{Cs}$ and 10.91 Å for the $\text{Zn}_2\text{Al}:\text{SO}_4/\text{Cs}$). Nevertheless, as indicated by the ICP-OES analyses (Table 2), although traces of cesium were found, the content of sulfate was lower, indicating that the formulas are attributed to regular LDHs ($[\text{M}^{2+}_{0.667}\text{Al}^{3+}_{0.333}(\text{OH})_2](\text{SO}_4)_{0.167}$).^{37,52}

The confirmation of the exchange reactions $\text{NO}_3^-/\text{SO}_4^{2-}$ can also be clearly seen by the replacement of the sharp bands at 1384 cm^{-1} (Figure 3Ba,c), attributed to nitrate, and appearance of bands in the region of 1100 cm^{-1} , attributed to sulfate (Figure 3Bb,d). This band split also indicated distorted sulfate symmetry. After the exchange reaction of $\text{Mn}_2\text{Al}:\text{NO}_3$ with Cs_2SO_4 , (Figure 3Ba,b), extra bands were also observed at 968 and 1026 cm^{-1} , which could be attributed to O–H bending modes, similar to those observed in gibbsite.⁵³ The same bands (although that at 968 cm^{-1} can be attributed to sulfate) were also observed for $\text{Mn}_2\text{Al}:\text{NO}_3$ and $\text{Mn}_2\text{Al}:\text{Cl}/\text{Cs}$ (indicated by *). The origin of these bands was not clearly understood. A small contamination of carbonate (band at 1362 cm^{-1}) was also observed in the sample $\text{Zn}_2\text{Al}:\text{NO}_3/\text{Cs}$ (Figure 3Bd),²⁸ already present as a shoulder in the sample $\text{Zn}_2\text{Al}:\text{NO}_3$ before the exchange reactions (Figure 3Bc). The presence of carbonate can explain the slightly lower content of sulfate (0.146 instead of 0.167) (Table 2).

After the exchange of chloride (Figure 3Be), the expected band appeared in the region of 1100 cm^{-1} , attributed to sulfate (Figure 3Bf). All the other bands remained constant, indicating the maintenance of the LDH lattice and suggesting exchange reactions of chloride with sulfate but without the incorporation of Cs^+ (Table 2). SEM images of some key synthesized samples (Figure 4) indicated the expected morphology of LDH, with platelet-like particles, in which the diameter varied according to the

compositions, being smaller than 1 μm in $\text{Mn}_2\text{Al}:\text{SO}_4/\text{Na}$ (Figure 4a) and $\text{Zn}_2\text{Al}:\text{SO}_4/\text{Na}$ (Figure 4b).

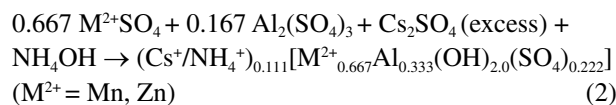
In the case of $\text{Mn}_2\text{Al}:\text{NO}_3$ (Figure 4c) and $\text{Mn}_2\text{Al}:\text{Cl}$ (Figure 4d), bigger particles were observed, reaching several micrometers with some powdered particles at the top of the crystals. These powdered particles are not attributed to crystalline impurities, since the XRD patterns indicated only basal peaks from the LDH, and chemical analysis also indicated the predicted composition (Table 2). The EDS spectra (Figures 4e–4h) also indicated qualitatively the presence of the expected elements according to the chemical compounds used during the synthesis.

As copper tapes were used to hold the samples, a small contamination with this element was observed in some of the spectra (indicated with asterisks).

All the compounds intercalated with hydrated sulfate in the presence of alkali metal cations, hydrated sulfate or even with grafted hydrated sulfate presented basal distances close to 11 Å (Figure 5), making them difficult to distinguish through XRD, but quantitative analysis by ICP-OES helped us to give some information about these complex systems.

Conclusions

LDH intercalated with Cs^+ and NH_4^+ together with SO_4^{2-} obtained by co-precipitation of sulfate salts with aqueous NH_3 in the presence of excess Cs_2SO_4 , presented the composition $(\text{Cs}/\text{NH}_4)_{0.111}[\text{M}^{2+}_{0.667}\text{Al}_{0.333}(\text{OH})_{2.0}(\text{SO}_4)_{0.222}]$ ($\text{M}^{2+} = \text{Mn}$ or Zn) (equation 2), attested by ICP-OES analyses, basal distances close to 11 Å in the XRD patterns and typical bands of SO_4^{2-} and NH_4^+ in the FTIR spectra.



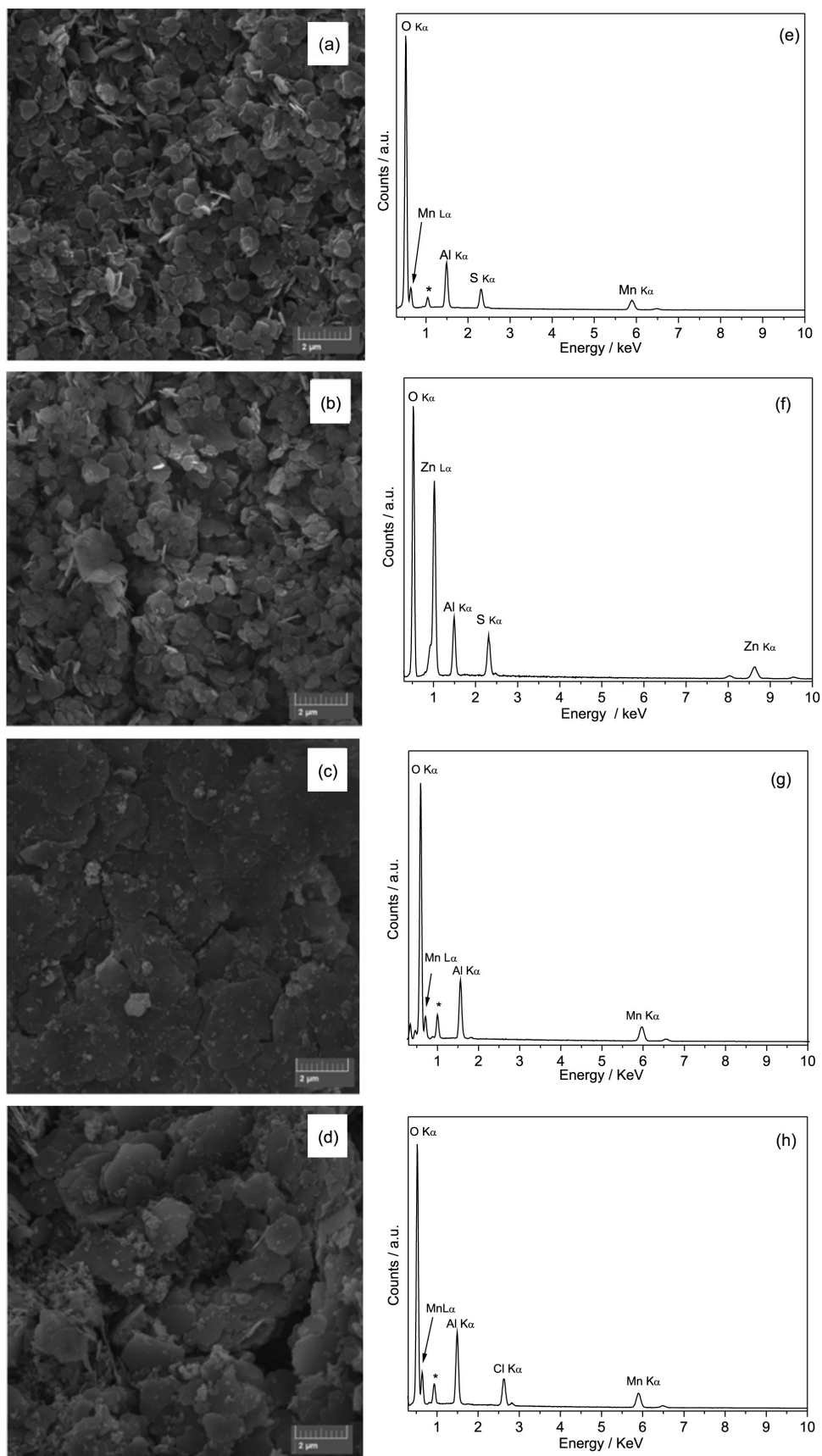


Figure 4. SEM images of $\text{Mn}_2\text{Al}:\text{SO}_4/\text{Na}$ (a), $\text{Zn}_2\text{Al}:\text{SO}_4/\text{Na}$ (b), $\text{Mn}_2\text{Al}:\text{NO}_3$ (c), $\text{Mn}_2\text{Al}:\text{Cl}$ (d) and the corresponding EDS spectra (e-h) (*Cu from the sample holder).

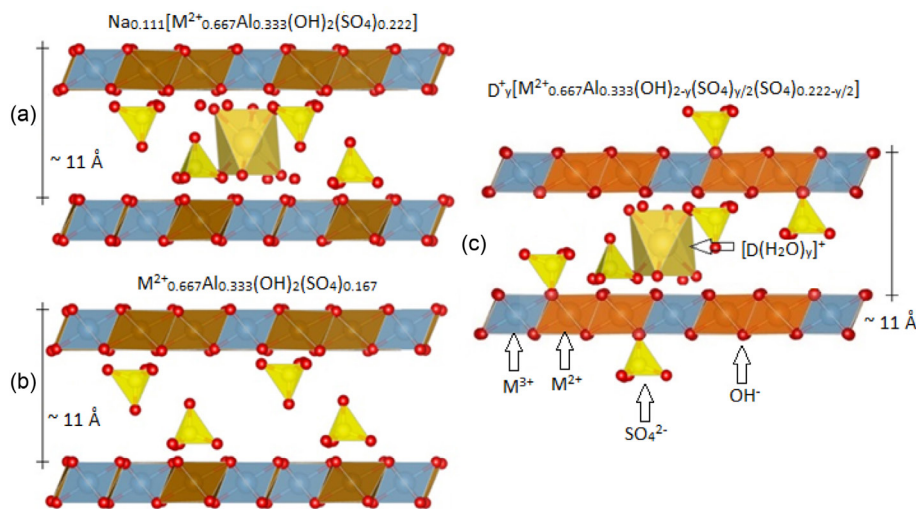
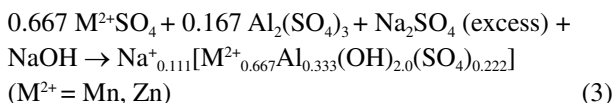
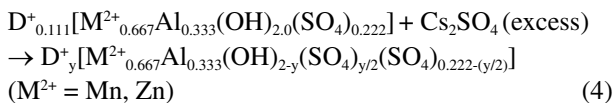


Figure 5. Schematic representation of the $2\text{M}^{2+}:\text{M}^{3+}$ LDH structures intercalated with hydrated $\text{Na}^+/\text{SO}_4^{2-}$, such as in shigaite (a),²⁸ hydrated SO_4^{2-} as in $[\text{Zn}_2\text{Cr}(\text{OH})_6](\text{SO}_4)_{0.5}\cdot 4\text{H}_2\text{O}$ (b)⁵⁴ and intercalated/grafted with SO_4^{2-} , as proposed in the present work (c). Water molecules were removed to facilitate visualization.

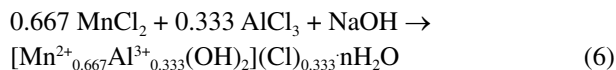
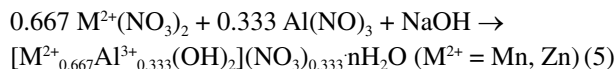
LDH synthesized by co-precipitation with increasing pH of sulfate salts with NaOH and excess of Na_2SO_4 presented the composition $\text{Na}_{0.111}[\text{M}^{2+}_{0.667}\text{Al}_{0.333}(\text{OH})_{2.0}(\text{SO}_4)_{0.222}]$ ($\text{M}^{2+} = \text{Mn}, \text{Zn}$) (equation 3), basal distances close to 11 Å and typical bands of SO_4^{2-} .



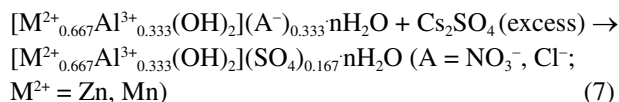
After putting $\text{Na}_{0.111}[\text{M}^{2+}_{0.667}\text{Al}_{0.333}(\text{OH})_{2.0}(\text{SO}_4)_{0.222}]$ in contact with excess Cs_2SO_4 in an attempt to exchange Na^+ with Cs^+ , the LDH containing $\text{SO}_4^{2-}/\text{Cs}^+$ obtained were compared to those obtained by direct co-precipitation with increasing pH. In these samples, the basal distance was also close to 11 Å, but Na^+ were partially exchanged with Cs^+ , while the amount of sulfate was constant, as attested by ICP-OES analyses and typical bands in the FTIR spectra, suggesting the formulas $\text{D}^+_y[\text{M}^{2+}_{0.667}\text{Al}_{0.333}(\text{OH})_{2-y}(\text{SO}_4)_{y/2}(\text{SO}_4)_{0.222-(y/2)}]$ (equation 4) ($\text{D}^+ = \text{Na}^+$ or Cs^+), where $(\text{SO}_4)_{y/2}$ represents grafted SO_4^{2-} , partially replacing the OH^- in the layers: $(\text{OH})_{2-y}$.



Co-precipitating nitrate or chloride salts with NaOH, compounds with the composition $[\text{M}^{2+}_{0.667}\text{Al}^{3+}_{0.333}(\text{OH})_2](\text{NO}_3)_{0.333}\cdot n\text{H}_2\text{O}$ ($\text{M}^{2+} = \text{Mn}, \text{Zn}$) were obtained (equations 5,6), having respective basal distances of 8.92 and 7.92 Å and presenting typical bands in the FTIR spectra.



After exchanging the samples intercalated with nitrate and chloride with Cs_2SO_4 in excess, the basal distance changed to around 11 Å and typical FTIR bands of SO_4^{2-} were observed, indicating the intercalation of SO_4^{2-} . But the content of cesium was very low, suggesting the maintenance of the formula $[\text{M}^{2+}_{0.667}\text{Al}^{3+}_{0.333}(\text{OH})_2](\text{SO}_4)_{0.167}\cdot n\text{H}_2\text{O}$ (equation 7), as also proposed by equation 1.



This is the first report in the literature of synthesis and characterization of LDHs intercalated with $\text{SO}_4^{2-}/\text{Cs}^+/\text{Na}^+$ or $\text{SO}_4^{2-}/\text{Cs}^+/\text{NH}_4^+$, opening new alternatives to remove radioactive nuclides from contaminated waters using LDHs obtained by co-precipitation syntheses with increasing pH.

Acknowledgments

We acknowledge funding from the Office to Coordinate Improvement of University Personnel (CAPES) - Finance Code 001 for the PhD scholarship of ARS; the National Council for Scientific and Technological Development (CNPq, grant 300988/2019-2); Financier of Studies and Projects (FINEP). We are also grateful to Prof Marco

Tadeu Grassi and MSc Mayara Padovan dos Santos for the ICP-OES analyses.

References

1. Cajipe, V. B.; Heiney, P. A.; Fischer, J. E.; *Phys. Rev. B* **1989**, *39*, 4374.
2. Paulus, W.; Katzke, H.; Schöllhorn, R.; *J. Solid State Chem.* **1992**, *96*, 162.
3. Messaoudi, A.; Conard, J.; Setton, R.; Beguin, F.; *Chem. Phys. Lett.* **1993**, *202*, 506.
4. Tonti, D.; Pettenkofer, C.; Jaegermann, W.; Papageorgopoulos, D. C.; Kamaratos, M.; Papageorgopoulos, C. A.; *Ionics* **1998**, *4*, 93.
5. Silipigni, L.; Acacia, N.; Quattrone, T.; de Luca, G.; Scolaro, L. M.; Salvato, G.; *J. Appl. Phys.* **2007**, *102*, 113713.
6. Park, C. W.; Kim, B. H.; Yang, H. M.; Seo, B. K.; Moon, J. K.; Lee, K. W.; *Chemosphere* **2017**, *168*, 1068.
7. Mao, Y. L.; Fang, Y. Q.; Pan, J.; Wang, D.; Bu, K. J.; Che, X. L.; Zhao, W.; Huang, F. Q.; *J. Solid State Chem.* **2019**, *279*, 120937.
8. Christiansen, B. C.; Dideriksen, K.; Katz, A.; Nedel, S.; Bovet, N.; Sørensen, H. O.; Frandsen, C.; Gundlach, C.; Andersson, M. P.; Stipp, S. L. S.; *Inorg. Chem.* **2014**, *53*, 8887.
9. Mukai, H.; Hirose, A.; Motai, S.; Kiruchi, R.; Tanoi, K.; Nakanishi, T. M.; Yaito, T.; Yaita, T.; Kogure, T.; *Sci. Rep.* **2016**, *21543*.
10. Naamen, S.; Jáafar, N.; Rhaïem, H. B.; Amara, A. B. H.; Plançon, A.; Muller, F.; *Clay Miner.* **2016**, *51*, 29.
11. Park, C. W.; Kim, S. M.; Kim, I.; Yoon, I. H.; Hwang, J.; Kim, J. H.; Yang, H. M.; Seo, B. K.; *J. Environ. Radioact.* **2021**, *233*, 106592.
12. *Clay Surfaces - Fundamentals and Applications*, vol. 1; Wypych, F.; Satyanarayana, K. G., eds.; Academic Press: Amsterdam, 2004.
13. *Layered Double Hydroxides*; Duan, X.; Evans, D. G., eds.; Springer Verlag: Berlin, 2006.
14. Wang, Q.; O'Hare, D.; *Chem. Rev.* **2012**, *112*, 4124.
15. Rives, V.; del Arco, M.; Martín, C.; *Appl. Clay Sci.* **2014**, *88-89*, 239.
16. Leroux, F.; Moujahid, E.; Taviot-Gueho, C.; Besse, J. P.; *Solid State Sci.* **2001**, *3*, 81.
17. Radha, A. V.; Kamath, P. V.; Shivakumara, C.; *Solid State Sci.* **2005**, *7*, 1180.
18. Williams, G. R.; Rees, N. H.; O'Hare, D.; *Solid State Sci.* **2009**, *11*, 1229.
19. Zhang, F. R.; Du, N.; Li, H. P.; Liu, J. Q.; Hou, W. G.; *Solid State Sci.* **2014**, *32*, 41.
20. Delmas, C.; Borthomieu, Y.; *J. Solid State Chem.* **1993**, *104*, 345.
21. Sotiles, A. R.; Wypych, F.; *Chem. Commun.* **2019**, *55*, 7824.
22. Sotiles, A. R.; Baika, L. M.; Grassi, M. T.; Wypych, F.; *J. Am. Chem. Soc.* **2019**, *141*, 531.
23. Sotiles, A. R.; Grassi, M. T.; dos Santos, M. P.; Wypych, F.; *J. Braz. Chem. Soc.* **2021**, *32*, 170.
24. Sotiles, A. R.; Wypych, F.; *Solid State Sci.* **2020**, *106*, 106304.
25. Rodgers, K. A.; Chisholm, J. E.; Davis, R. J.; Nelson, C. S.; *Mineral. Mag.* **1977**, *41*, 389.
26. Zamareno, I.; Plana, F.; Vazques, A.; Clague, D. A.; *Am. Mineral.* **1989**, *74*, 1054.
27. Witzke, T.; Pöllmann, H.; Vogel, A.; *Z. Kristallogr.* **1995**, *9*, S.252.
28. Cooper, M. A.; Hawthorne, F. C.; *Can. Mineral.* **1996**, *34*, 91.
29. Huminicki, D. M. C.; Hawthorne, F. C.; *Can. Mineral.* **2003**, *41*, 79.
30. Christiansen, B. C.; Balic-Zunic, T.; Petit, P. O.; Frandsen, C.; Mørup, S.; Geckeis, H.; Katerinopoulou, A.; Stipp, S. L. S.; *Geochim. Cosmochim. Acta* **2009**, *73*, 3579.
31. Mills, S. J.; Christy, A. G.; Genin, J. M. R.; Kameda, T.; Colombo, F.; *Mineral. Mag.* **2012**, *76*, 1289.
32. Constantino, V. R. L.; Pinnavaia, T. J.; *Inorg. Chem.* **1995**, *34*, 883.
33. Radha, S.; Jayanthi, K.; Breu, J.; Kamath, P. V.; *Clays Clay Miner.* **2014**, *62*, 53.
34. Persson, I.; *Pure Appl. Chem.* **2010**, *82*, 1901.
35. Brugé, F.; Bernasconi, M.; Parrinello, M.; *J. Am. Chem. Soc.* **1999**, *121*, 10883.
36. Guo, J.; Zhou, L.; Zen, A.; Michaelides, A.; Wu, X.; Wang, E.; Xu, L.; Chen, J.; *Phys. Rev. Lett.* **2020**, *125*, 106001.
37. Khaldi, M.; de Roy, A.; Chaouch, M.; Besse, J. P.; *J. Solid State Chem.* **1997**, *130*, 66.
38. Pironon, J.; Pelletier, M.; de Donato, P.; Mosser-Ruck, R.; *Clay Miner.* **2003**, *38*, 201.
39. Aranda, P.; Ruiz-Hitzky, E.; *Appl. Clay Sci.* **1999**, *15*, 119.
40. Nakamoto, K.; *Infrared and Raman Spectra of Inorganic and Coordination Compounds, Part A: Theory and Applications in Inorganic Chemistry*, 5th ed.; Wiley: New York, 1997.
41. Iftekhar, S.; Küçük, M. E.; Srivastava, V.; Repo, E.; Sillanpa, M.; *Chemosphere* **2018**, *209*, 470.
42. Adiwidjaja, G.; Friese, K.; Klaska, K. H.; Schlüter, J.; *Z. Kristallogr.* **1997**, *212*, 704.
43. Maruyama, S. A.; Krause, F.; Tavares, S. R.; Leitão, A. A.; Wypych, F.; *Appl. Clay Sci.* **2017**, *146*, 100.
44. Hawthorne, F. C.; Kimata, M.; Eby, R. K.; *Am. Mineral.* **1993**, *78*, 649.
45. Bindi, L.; Christy, A. G.; Mills, S. J.; Ciriotti, M. E.; Bittarello, E.; *Can. Mineral.* **2015**, *53*, 791.
46. Witzke, T.; Raade, G.; *Neues Jahrb. Mineral., Monatsh.* **2000**, *455*.
47. Nickel, E. H.; Graham, J.; *Can. Mineral.* **1987**, *25*, 409.
48. Zegeye, A.; Ona-Nguema, G.; Carteret, C.; Huguet, L.; Abdelmoula, M.; Jorand, F.; *Geomicrobiol. J.* **2005**, *22*, 389.

49. Marappa, S.; Radha, S.; Kamath, P. V.; *Eur. J. Inorg. Chem.* **2013**, *12*, 2122.
50. Bookin, A. S.; Drits, V. A.; *Clays Clay Miner.* **1993**, *41*, 551.
51. Pachayappan, L.; Kamath, P. V.; *Clays Clay Miner.* **2019**, *67*, 154.
52. Radha, S.; Antonyraj, C. A.; Kamath, P. V.; Kannan, S.; *Z. Anorg. Allg. Chem.* **2010**, *636*, 2658.
53. Balan, E.; Lazzeri, M.; Morin, G.; Mauri, F.; *Am. Mineral.* **2006**, *91*, 115.
54. Radha, S.; Kamath, P. V.; *Inorg. Chem.* **2013**, *52*, 4834.

Submitted: July 6, 2021

Published online: September 9, 2021

